Korean J. Chem. Eng., 39(5), 1339-1349 (2022)
DOI: 10.1007/s11814-021-1012-0

pISSN: 0256-1115
eISSN: 1975-7220

Roasting and leaching process of iron sulfate to separate zinc and iron from blast furnace dust

Ruimeng Shi*, Hao Wu*,,***,†, Huan Liu*, Bixia Wang*, Yuan She*, Chong Zou*,†, Jiangfeng Zheng**,***, and Qi Gao**,***

*School of Metallurgical Engineering, Xi'an University of Architecture and Technology, Xi'an 710311, China
**Guangdong Jiana Energy Technology Co. Ltd, Qingyuan 513056, China
***Qingyuan Jiazhi New Materials Research Institute Co. Ltd., Qingyuan, 511517, China
(*Received 1 June 2021 • Revised 2 November 2021 • Accepted 10 November 2021*)

Abstract−The physical phase analysis and thermodynamic calculations of blast furnace dust were performed using X-ray diffraction fluorescence spectrometer, X-ray diffractometer, scanning electron microscope, energy spectrometer, and Factsage software. The leaching pattern and mechanism of zinc elements were studied by a roasting-leaching method. The results showed that the conversion of zinc ferrite to zinc sulfate could be realized when the roasting temperature range was 500-730 °C, which was convenient for zinc leaching. A better roasting condition could be obtained when the roasting temperature was 600 °C, roasting time was 60 min, and molar ratio of ferric sulfate was 1.2 : 1. Under these conditions, the zinc and iron leaching rates were 84.57% and 24.51%, respectively, at a sulfuric acid concentration of 110 gL^{-1}, liquid-solid ratio of 10 : 1 mLg^{-1}, leaching time of 60 min, stirring speed of 400 rpm, and leaching temperature of 80 °C. The leaching process of zinc from blast furnace dust sulfate roasting products agreed with the unreacted core model, and internal diffusion was the restrictive step. The kinetic equation of the leaching process was $1-2R/3-(1-R)^{2/3}=0.47t$, the apparent activation energy of the leaching reaction was 17.4 $kJmol^{-1}$, and the reaction order was 1.908.

Keywords: Blast Furnace Dust, Thermodynamic Analysis, Sulfate Roasting, Leaching Conditions, Kinetics

INTRODUCTION

As the iron and steel industry develops rapidly, and the crude steel output increases yearly, the smelting process will produce much dust. Blast furnace ironmaking is the primary source of iron in dust, which is mainly discharged from the top of a blast furnace with high-temperature gas in the high-temperature smelting process of the blast furnace, accounting for about 8-12% of the total steel output [1]. In addition to iron, dust also contains C, Zn, Ti, Mn, Zr, Pb, As, Cd, and other metallic elements [2]. However, because of the different raw materials and processes of enterprises, the content of elements in blast furnace dust (BFD) differs [3]. To save costs, some enterprises directly return BFD to the blast furnace for sintering [4]; alternatively, it can be recycled after treatment by pelletization [5,6]. As a major metal element in BFD (after iron), zinc will reduce the service life of a blast furnace and cause certain harm to blast furnace smelting if it is not controlled in the raw material and cyclic enrichment in the blast furnace [7] At present, zinc in BFD is mainly extracted by pyrometallurgy or hydrometallurgy process, but these single methods have a low separation degree and a high metal loss rate [8,9]. Untreated, BFD will cause environmental pollution and resource wastage. The separation of zinc and iron in a BFD via a proper process is significant to the comprehensive recovery and usage of valuable resources in the BFD and the reduction of the production cost.

At present, BFD treatments vary because of different zinc content. For BFD with low zinc content, landfill or enrichment method is mainly adopted [10,11]; however, the landfill method cannot realize the recovery and usage of valuable metal resources in dust, and the enrichment method has high equipment cost and low economic value, which can generally be resolved by ore blending in the actual process. Dust with high zinc content is usually treated by pyrometallurgy, hydrometallurgy, or combined pyrometallurgy-hydrometallurgy process. After the raw material is mixed with a reducing agent, zinc oxide is reduced to gaseous elemental zinc at a high temperature. Zinc volatilizes into smoke dust at high temperature, and zinc oxide is obtained through secondary oxidation enrichment. The common secondary oxidation enrichment methods include pelletizing treatment [12], rotary kiln process [13-15], rotary bottom furnace process [16], circulating fluidized bed process [17], and melting reduction process [18-20]. Although these processes are simple, the raw material adaptability is strong, the equipment is costly, and the maintenance is difficult, the process energy consumption is relatively high, but the composition of the raw material is not high, the processing temperature is high, and the material and energy consumption is large. According to the different leaching solutions used, the process of hydrometallurgy treatment of zinc-containing metallurgical dust can be mainly divided into acid, alkali, and ammonia leaching methods [21-23]. However, zinc in BFD usually exists as stable zinc ferrite. For low zinc dust, the conventional hydrometallurgy acid leaching directly results in a low zinc leaching rate. If high temperature and high acid leaching are performed, the zinc leaching rate will significantly increase, but iron will dissolve into the solution, increasing the cost of the

†To whom correspondence should be addressed.
E-mail: whyk20151121@163.com, zouchong985@163.com

subsequent iron removal process [21]. In addition, equipment corrosion is serious and difficult to operate and control, and the processing easily produces sulfur, chlorine, and other products that pollute the environment. Combined recovery of zinc and iron from $ZnFe_2O_4$ possesses certain advantages and is widely used. SO_2 direct conversion of $ZnFe_2O_4$ after using water leaching-magnetic separation can obtain high elemental leaching rate and convenient and pollution-free [24]; zinc-iron slag and pyrite roasting after using magnetic separation and flotation can separate zinc and iron with high sulfide rate and iron concentrate grade [25,26]. Zinc in BFD mainly exists in zinc ferrite, which has stable chemical properties and is difficult to treat by conventional methods [27]. The combined treatment of BFD can convert zinc ferrite into zinc oxide with remarkable effects. The roasting temperature is in the range of 900-1,350 °C, and the hydrometallurgy treatment can achieve a leaching rate of more than 90% [28]. However, direct high-temperature roasting will volatilize harmful metals in dust and pollute the environment. Strong alkali sintering can convert zinc ferrite into sodium ferrite and iron oxide, and then hydrometallurgy leaching. The zinc leaching rate is significantly improved [29,30], but in the leaching process, a large amount of acid will be consumed to neutralize excessive alkali, and chloride ions will be introduced to the entire system. Reduction roasting and reducing atmosphere roasting can also improve zinc leaching rate [31,32], but the reducing atmosphere poses certain dangers in the industry, and the price of pure solid reducing agent is expensive. Selecting a low-cost additive to ensure the degradation of zinc ferrite is a paramount technique to separate iron and zinc in BFD without introducing other impurities in the leaching process.

Referring to the separation method of zinc and iron from hydrometallurgical zinc slag, the combined pyrometallurgy-hydrometallurgy process was employed to treat BFD. The physical properties of BFD were studied by X-ray diffraction fluorescence spectrometry (XRF), X-ray diffractometry (XRD), and scanning electron microscopy (SEM). A stable zone diagram of the Zn-Fe-S-O system was drawn by selecting ferric sulfate as an additive. The thermodynamic conditions for the transformation of zinc ferrite into soluble zinc sulfate in BFD were analyzed. The effects of roasting temperature, ferric sulfate ratio, and roasting temperature on the leaching rates of zinc and iron from BFD were studied. The effects of sulfuric acid concentration, leaching temperature, liquid-solid ratio, and leaching time on iron and zinc leaching rates were studied through single-factor experiments. A better separation process of zinc and iron from BFD was obtained. The leaching kinetics of zinc was calculated using an unreacted core model, and the effects of leaching temperature and leaching acidity on the reaction rate were studied, which provided a theoretical and technological reference for separating iron and zinc from BFD.

EXPERIMENT AND METHOD

1. Characterization of the BFD

The raw material used in the experiment was a BFD from a steel enterprise. The BFD was put into an oven and dried for 12 h at 105 °C to remove excess moisture. The dried sample was ground with a mortar to make the dust particles below 74 μm account for more than 90%. The elemental composition and content of BFD were analyzed via XRF. The results of the main components are shown in Table 1.

Table 1. Analysis results of main chemical components of BFD (%)

Fe	Zn	Si	Ca	Cl	S	Pb	Al	K
58.43	7.68	3.64	3.53	3.11	2.47	1.63	1.01	0.45

From Table 1, the main chemical elements in BFD are Fe, Zn, Si, Ca, Cl, and S.

2. Ferric Sulfate Roasting

The composition and mineral phase composition of BFD were obtained by XRF and XRD analyses. The existing forms of Zn in BFD were thermodynamically calculated using Factsage software. The change of standard Gibbs free energy in the roasting process of adding iron sulfate to the phase containing zinc was analyzed, and an optimum roasting temperature was obtained through analysis.

After the BFD and ferric sulfate were fully mixed according to a molar ratio of 1.2 : 1, the roasting experiment was performed in a muffle furnace at 640 °C for 60 min.

The specific steps of the experiment are as follows. Weed a certain amount of screened BFD and ferric sulfate powder, mix it evenly in a certain proportion, put a certain amount of powder in the mold, press it into cylindrical flakes with a table powder tablet press, and spread out the flakes into a corundum crucible with a lid to expand the reaction area of the sample and ensure that the sample can be fully roasted. The covered corundum crucible is placed at the center of the muffle furnace and the BFD is roasted at a set temperature and time. After calcining, the muffle furnace is shut off when the temperature in the furnace cools below 100 °C, then the furnace door is opened, and the samples taken out. The roasted sample is ground with a mortar, screened to less than 200 mesh, and stored in a sample bag for subsequent leaching and analysis.

3. Acid Leaching Experiments

We weighed a certain amount of roasted BFD into a 500-mL beaker, added a leaching agent (sulfuric acid), and performed the leaching experiment in a constant temperature water bath. After leaching, a circulating vacuum pump was used to filter the leaching liquid. The leaching residue was washed with distilled water, dried, weighed, and analyzed.

The chemical composition of BFD was analyzed by an S4Pioneer X-ray fluorescence spectrometer. XRD (D8 ADVANCE A25) was used to analyze the phase composition of dust, calcined products, and leachate. The determination conditions were as follows: a Cu target Kα ray, 40-kV tube voltage, 250-mA tube current, 20-900 scanning range, and 3°/min step length. The microscopic morphologies of dust, calcined products, and leached residues were analyzed by Geminis EM300.

The content of zinc and iron in dust, roasting products, and leaching residues were analyzed by chemical titration, and the leaching rate was calculated [10,33].

RESULTS AND DISCUSSION

1. Raw Material Analysis

The chemical composition of BFD was analyzed by XRD to deter-

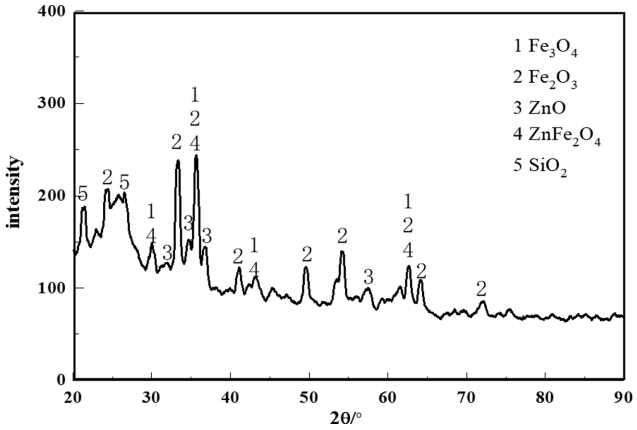

Fig. 1. Phase analysis of BFD (XRD).

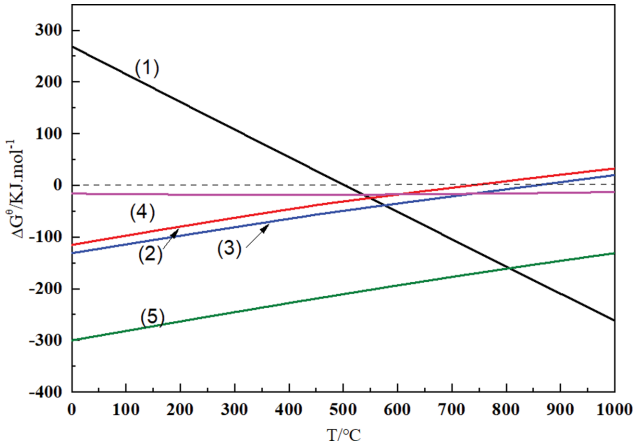

Fig. 3. ΔG^{θ}-T curve of reactions during roasting.

mine the main phase composition of BFD. The analysis results are shown in Fig. 1.

From Fig. 1, the BFD primarily comprises Fe_3O_4, Fe_2O_3, $ZnFe_2O_4$, and limonite. Zinc ferrite is a substance with a stable spinel structure, which is generated by the reaction of zinc oxide and ferrous oxide in high-temperature conditions and is difficult to be leached by conventional methods, resulting in a low zinc leaching rate [27]. Therefore, it is necessary to decompose the zinc ferrite in the BFD to recover the zinc.

SEM and electron energy spectrometry (SEM-EDS) was used to detect and analyze the morphology of BFD (Fig. 2). From Fig. 2, the BFD particles have rough surfaces, uneven sizes, and different shapes. They mainly comprise strips, rhomboids, and irregularly shaped particles, and there is encapsulation, agglomeration, and Mosaic phenomena among the particles.

When the BFD is roasted with iron sulfate, the possible reactions of the main components in the roasting process are as follows:

$$Fe_2(SO_4)_3=Fe_2O_3+3SO_3 \quad (1)$$

$$ZnFe_2O_4+SO_3=ZnSO_4+Fe_2O_3 \quad (2)$$

$$ZnO+SO_3=ZnSO_4 \quad (3)$$

$$ZnO+Fe_2O_3=ZnFe_2O_4 \quad (4)$$

$$CaO+SO_3=CaSO_4 \quad (5)$$

Factsage software was used to calculate the standard Gibbs free energy variation (ΔG^{θ}) of the above reactions in the temperature range of 0-1,000 °C, and the ΔG^{θ}-T curve was drawn (Fig. 3).

From Fig. 3, the ΔG^{θ} of reaction (1) decreased gradually with an increase in temperature. When the temperature increased to 500 °C, the reaction could proceed spontaneously. The results showed that the decomposition reaction of ferric sulfate would occur when

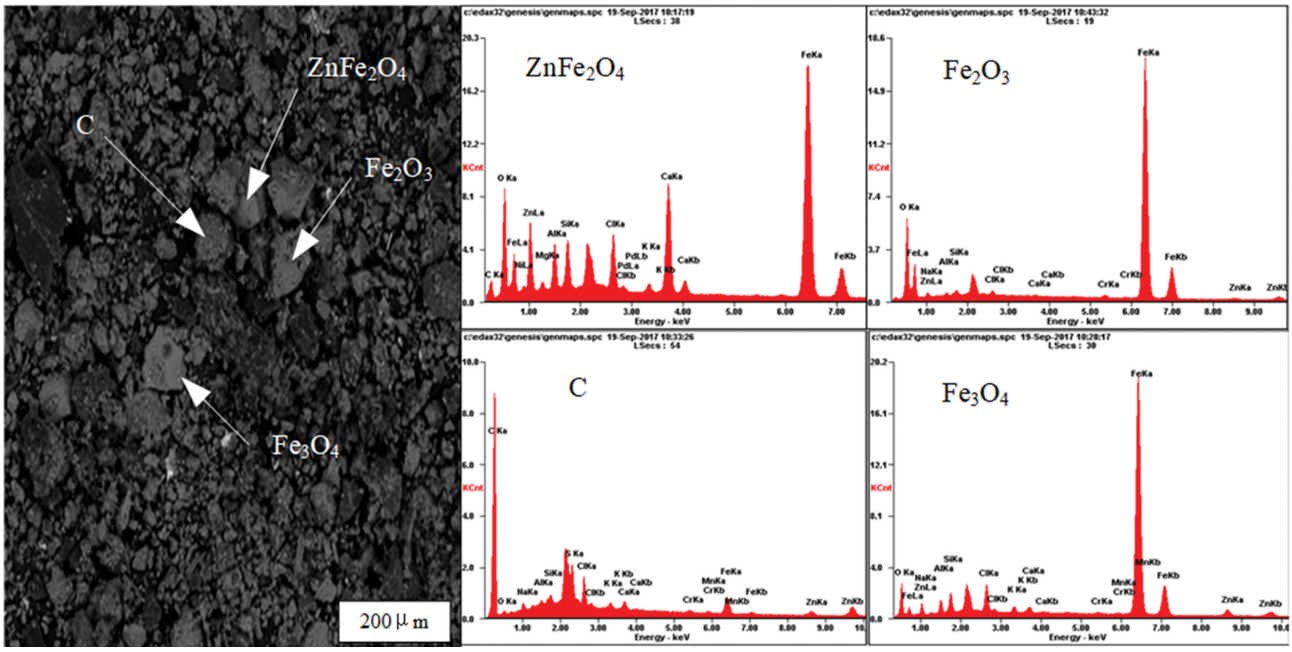

Fig. 2. SEM-EDS analysis of BFD.

the reaction temperature increased to 500 °C in the standard condition, resulting in the formation of ferric oxide and sulfur trioxide, and increasing the temperature could induce this reaction. The ΔG^{θ} of reaction (2) increased gradually with an increase in temperature. When the temperature was higher than 750 °C, the reaction could not occur spontaneously, and extremely high temperatures were unconducive to the decomposition of zinc ferrite to zinc sulfate. From 0-1,000 °C, the standard Gibbs free energy change of reaction (4) was always negative, and its ΔG^{θ} decreased gradually with an increase in temperature, indicating that the reaction of synthesis of zinc ferrite from iron oxide and zinc oxide could occur spontaneously, and the increase in temperature promoted the reaction. Combining the curves of reactions (3) and (4) and the calculated values of ΔG^{θ} of each reaction, reaction (3) would probably occur when the temperature was lower than about 730 °C. If the temperature was higher than 730 °C, the reaction would probably produce zinc ferrite. Therefore, to reduce the synthesis of zinc ferrite in the roasting process, the roasting temperature should be controlled below 730 °C. The ΔG^{θ} of reaction (5) was always negative in the temperature range of 0-1,000 °C and showed an increasing trend with increasing temperature, indicating that the formation of calcium sulfate could occur spontaneously and would probably occur instead of reaction (2). The generation of calcium sulfate would consume the sulfur trioxide produced by the decomposition of iron sulfate as well as reduce the decomposition rate of zinc

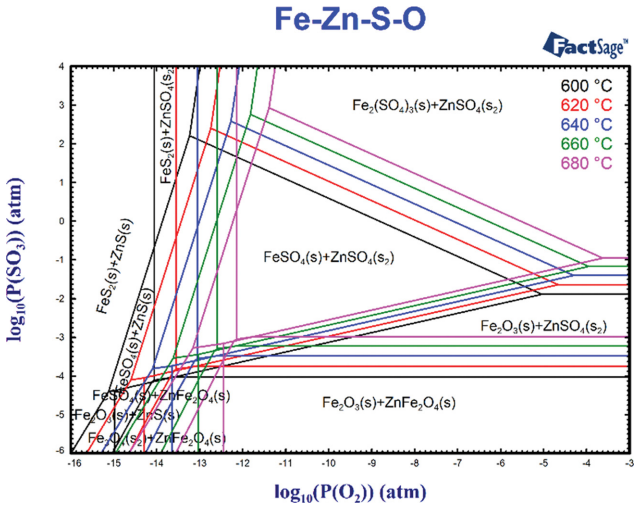

Fig. 4. Predominance area for the Zn-Fe-S-O system within 600-680 °C.

ferrite. Therefore, the ratio of iron sulfate should be appropriately increased according to the content of calcium oxide in BFD during roasting to avoid an incomplete reaction of zinc ferrite. To further analyze the influence of temperature on BFD sulfate roasting, Factsage software was used to draw the regional dominance dia-

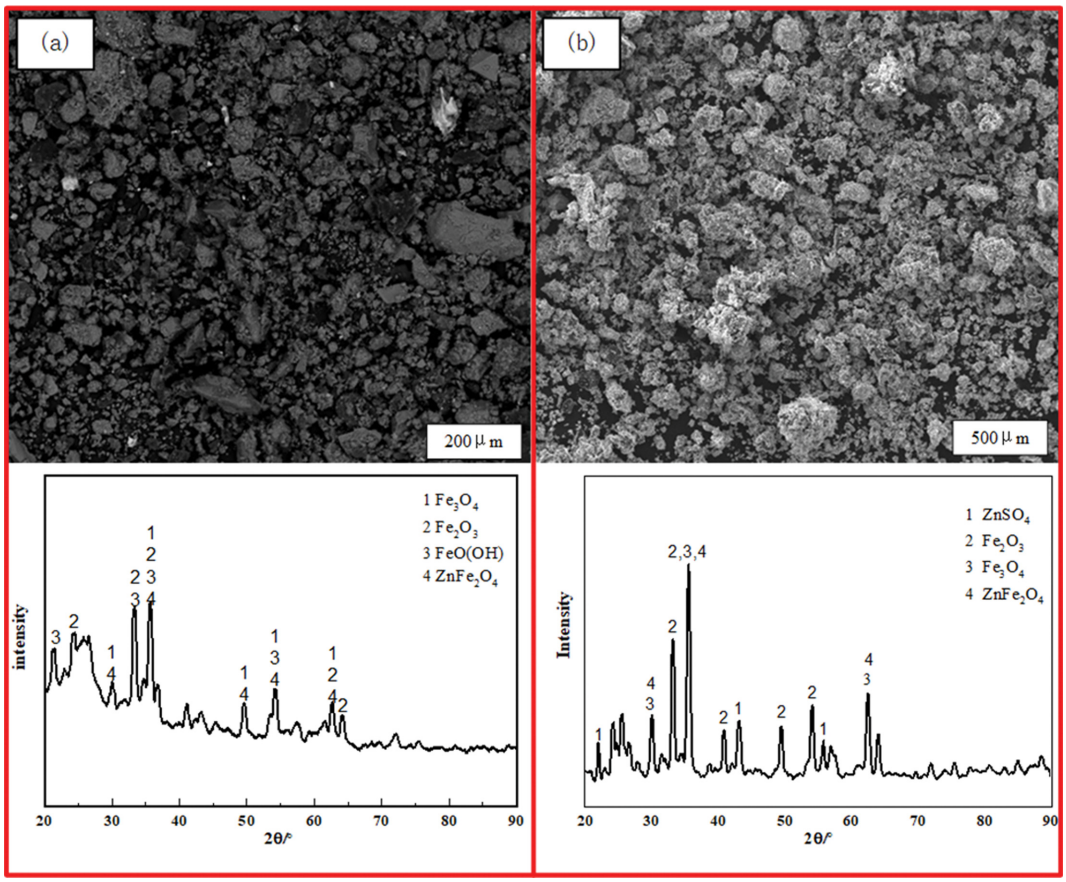

Fig. 5. Surface morphology and phase transformation of BFD roasting process: (a) before roasting and (b) after roasting.

gram of various substances of the Zn-Fe-S-O system in the range of 600-680 °C. The results are shown in Fig. 4.

From Fig. 4, from 600-680 °C, the phase regions of the sulfated reaction products of zinc ferrate mainly included $ZnSO_4$+Fe_2O_3, $ZnSO_4$+$ZnFe_2O_4$, ZnO+$ZnFe_2O_4$, $ZnSO_4$+$Fe_2(SO4)_3$, and $ZnSO_4$+$FeSO_4$. With the increase of temperature, the stable zone of $ZnSO_4$+Fe_2O_3 decreases gradually, which indicates that increasing temperature can inhibit the sulfation reaction of zinc ferrite under the condition of a certain proportion of atmosphere.

2. Feasibility Analysis

2-1. Surface Morphology and Phase Transformation during Roasting

After the BFD and ferric sulfate were fully mixed according to the molar ratio of 1.2 : 1, a roasting experiment was performed in the muffle furnace at 640 °C for 60 min. The SEM and XRD data of the samples before and after roasting are shown in Fig. 5.

From Fig. 5, BFD particles were finer, darker, and smoother than sulfate roasted products. After roasting, the particles of the sample were larger and the surface was rougher, because the products generated from the BFD were wrapped on the surface of the dust particles after the sulfate roasting reaction, making the dust particles agglomerate and grow. The results of XRD showed that the main phase compositions of the calcined product were zinc sulfate, iron oxide, and zinc ferrite. Compared with the phase diagram of the unroasted BFD, although the characteristic peak of $ZnSO_4$ appeared in the products after roasting, there was still zinc ferrite, indicating that most zinc ferrite in the BFD could be transformed into zinc sulfate by sulfate roasting.

2-2. Leaching Test of Roasting Products

To further study the effect of BFD sulfate roasting, without BFD and product roasting under the same acid leaching conditions, the concentration of sulfuric acid of 60 gL^{-1}, leaching temperature of 80 °C, leaching time of 60 min, liquid-solid ratio of 10 : 1 mL g^{-1}, speed of 400 rpm, before and after roasting of zinc and iron leaching rate of change are shown in Fig. 6.

From Fig. 6, the leaching rate of zinc and iron significantly increased after sulfate roasting; the leaching rate of zinc increased more significantly from 30.48% to 69.3%, whereas the leaching rate of iron only increased by 6.13%. Combined with XRD phase analysis, the result showed that sulfate roasting in the BFD of refractory zinc ferrite transformed into soluble zinc sulfate; increasing the leaching rate of zinc, iron in most calcined products exists in the form of iron oxide, and compared with zinc sulfate, ferric oxide dissolved slowly in the dilute sulfuric acid; the leaching rate increase is not particularly evident to achieve the goal of zinc and iron separation.

In conclusion, it is an effective strategy to realize the resource

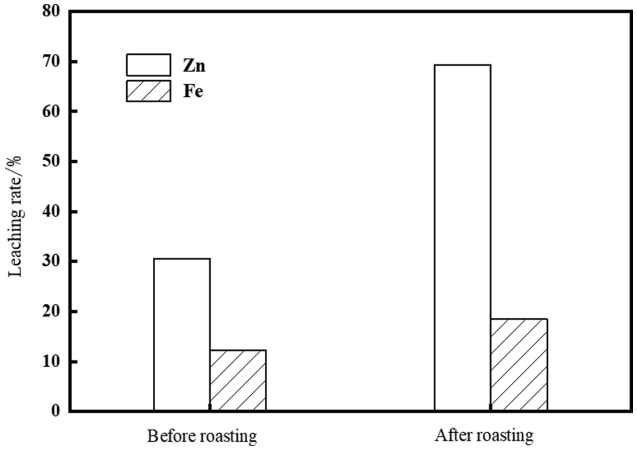

Fig. 6. Changes in leaching rate of zinc and iron before and after roasting; the concentration of sulfuric acid is 60 g L^{-1}, leaching temperature is 80 °C, leaching time is 60 min, liquid-solid ratio is 10 : 1 mL g^{-1}, and speed is 400 rpm.

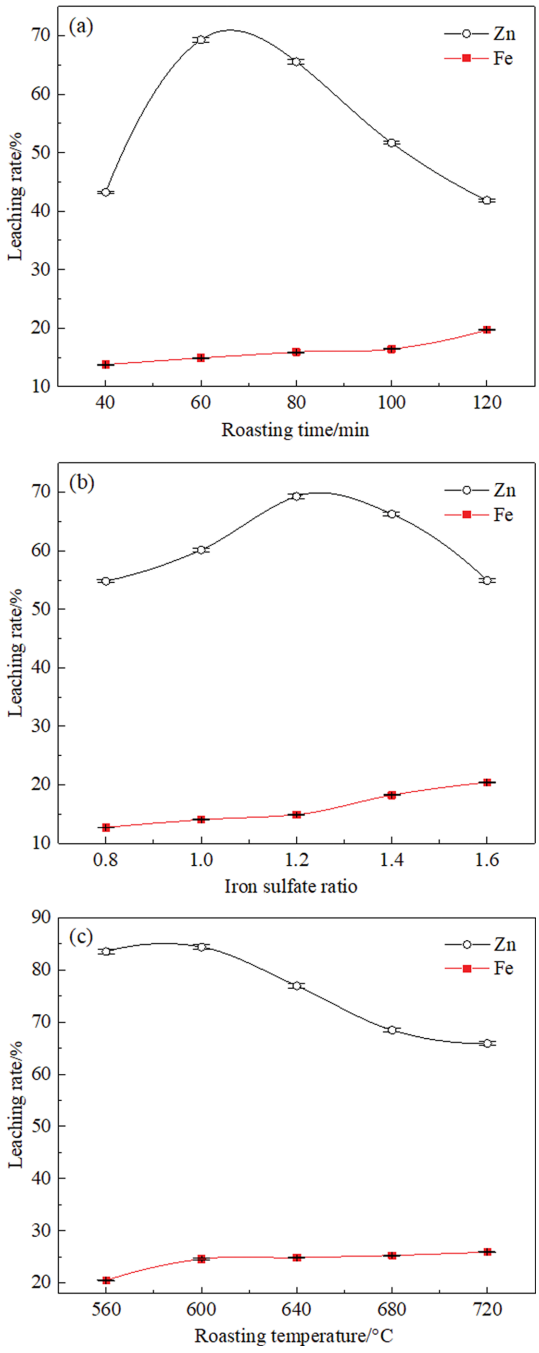

Fig. 7. Influence of zinc and iron leaching rate in BFD under different roasting conditions.

usage of BFD by a roasting process to convert $ZnFeO_4$ into soluble $FeSO_4$ to separate zinc and iron from BFD.

3. Influence of Roasting Conditions on the Leaching Rate of Zinc and Iron

To further investigate the effect of roasting conditions on the separation of zinc and iron, single-factor experiments were conducted to study the effects of roasting time, iron sulfate dosage, and roasting temperature on the leaching efficiency of iron and zinc from BFD, taking the leaching rate of zinc and iron from roasting products as the index. The leaching conditions of fixed roasting products were as follows: leaching acidity of 60 gL^{-1}, leaching temperature of 80 °C, liquid-solid ratio of 10 : 1 mL g^{-1}, and rotational speed of 400 rpm. The leaching results are shown in Fig. 7.

Fig. 7(a) The effects of roasting times (40, 60, 80, 100, and 120 min) on zinc and iron leaching rate were investigated at the roasting temperature of 640 °C and the ratio of ferric sulfate was 1.2 : 1. (b). Under the conditions of a roasting temperature of 640 °C and roasting time of 60 min, the changes in the leaching rate of zinc and iron in the roasting products were investigated when the molar ratios of ferric sulfate to zinc ferrite were 0.8 : 1, 1 : 1, 1.2 : 1, 1.4 : 1, and 1.6 : 1. (c). The effects of roasting temperature (560 °C, 600 °C, 640 °C, 680 °C, and 720 °C) on the zinc and iron leaching rate from sulfate roasting products were investigated under the conditions of a roasting time of 60 min and a molar ratio of ferric sulfate to zinc ferrite of 1.2 : 1.

From Fig. 7(a), the roasting time slightly influenced iron, but had a more obvious effect on zinc. With an increase in roasting time, the zinc leaching rate first increased from 43.22% to 69.3% and then decreased. After the roasting time was 60 min, the zinc leaching rate continued to decrease, and the iron leaching rate of iron increased continuously. When the roasting time was 120 min, the iron leaching rate was the highest, reaching 19.68%, which was because with the extension of roasting time, the added ferric sulfate would be gradually consumed, the amount of zinc sulfate generated gradually increased, and the zinc leaching rate improved. If the roasting time was prolonged, the ferric sulfate completely decomposed and no longer produced sulfur trioxide, i.e., it would be difficult to generate zinc sulfate. From the thermodynamic analysis in Fig. 4, the generation of zinc ferrite was inevitable in the roasting process, and the generation of zinc ferrite increased with the prolonging of time. When the total amount of zinc was certain, the content of soluble zinc decreased, resulting in a lower zinc leaching rate. To make the zinc in the calcination products dissolve considerably, the optimal calcination time was 60 min.

From Fig. 7(b), with an increase in the proportion of iron sulfate, the zinc leaching rate first increased and then decreased, whereas the iron leaching rate increased continuously. When the molar ratio of ferric sulfate to zinc ferrite was 1.2 : 1, the maximum zinc leaching rate was 69.3%, and that of iron was 14.89%. When the content of ferric sulfate reached a certain level, more Fe_2O_3 was generated, and the leaching rate of iron increased as the ratio of ferric sulfate continued to increase. Excessive Fe_2O_3 caused the reverse process of the reaction as well as promoted the formation of zinc ferrite, and the generation of zinc sulfate decreased accordingly, thereby decreasing the zinc leaching rate. After comprehensive consideration, the molar ratio of ferric sulfate to zinc ferrite was 1.2 : 1.

From Fig. 7(c), the roasting temperature significantly influenced the zinc leaching rate. With an increase in roasting temperature, the zinc leaching rate showed a trend of first increasing and then decreasing. When the temperature was lower than 600 °C, the zinc leaching rate increased with the roasting temperature, and the zinc leaching rate reached the highest at 600 °C, which was 84.37%. When the roasting temperature was higher than 600 °C, the zinc and iron leaching rates decreased with an increase in roasting temperature. Combined with thermodynamic analysis, the generation of zinc ferrite was inevitable during roasting, and the increase in temperature was conducive to the generation of zinc ferrite but unconducive to the conversion of zinc ferrite to zinc sulfate. Therefore, if the roasting temperature was too high, the conversion process of zinc ferrite was inhibited, and the zinc leaching rate decreased. To dissolve more zinc in BFD, the temperature of sulfate roasting should be selected as 600 °C.

4. Study of the Leaching Process of Dust Roasting Products

After sulfate roasting of BFD, it is necessary to separate zinc and iron by sulfuric acid leaching. This section focuses on the leaching process of BFD sulfate roasting product, analyzing the calcined product phase and the change in morphology before and after leaching by single-factor experiments. By inspecting the influence of leaching temperature, leaching time, leaching liquid acidity, and liquid-solid ratio on product roasting of zinc and iron leaching rates, the optimum leaching conditions were determined (Fig. 8).

Fig. 8(a) shows the effect of sulfuric acid concentration on the zinc and iron leaching rates from sulfate roasting of BFD. From Fig. 8(a), the increase of sulfuric acid concentration could promote the leaching of both zinc and iron from the products of BFD sulfate roasting, and the influence trend on iron was more obvious. With the increase in acidity from 80 to 100 gL^{-1}, the leaching rate of zinc increased from 72.1% to 76.75%, and that of iron increased from 15.46% to 19.14%. When the acidity was 110 gL^{-1}, the leaching rate of zinc reached the maximum, 76.94%. Afterward, with the further increase in acidity, the zinc leaching rate changed slightly, whereas the iron leaching rate showed an obvious increasing trend. The appropriate concentration of acid could make the zinc in the roasting product leach, and the iron remaining in the slag to separate zinc and iron. When the acid concentration was too high, the zinc content in the leach solution did not increase but caused too much iron content in the leach solution, increasing the burden of the subsequent iron sedimentation process. Therefore, the optimal leaching acidity to meet the conditions of high zinc content and low iron content in the leaching solution was 110 gL^{-1}.

Fig. 8(b) shows the influence of leaching time on the leaching rate of zinc and iron from the products of BFD sulfate roasting. From Fig. 8(b), when the leaching time was extended from 30 to 60 min, the zinc and iron leaching rates increased significantly. When the leaching time was 60 min, the maximum zinc leaching rate reached 76.94%; then, with the extension of the leaching time, the zinc and iron leaching rate tended to be flat because, with the leaching process, the soluble zinc and iron oxide in the roasting products were all added to the leaching solution so that the zinc and iron leaching rates significantly increased, whereas the other insoluble substances were still retained in the leaching residue.

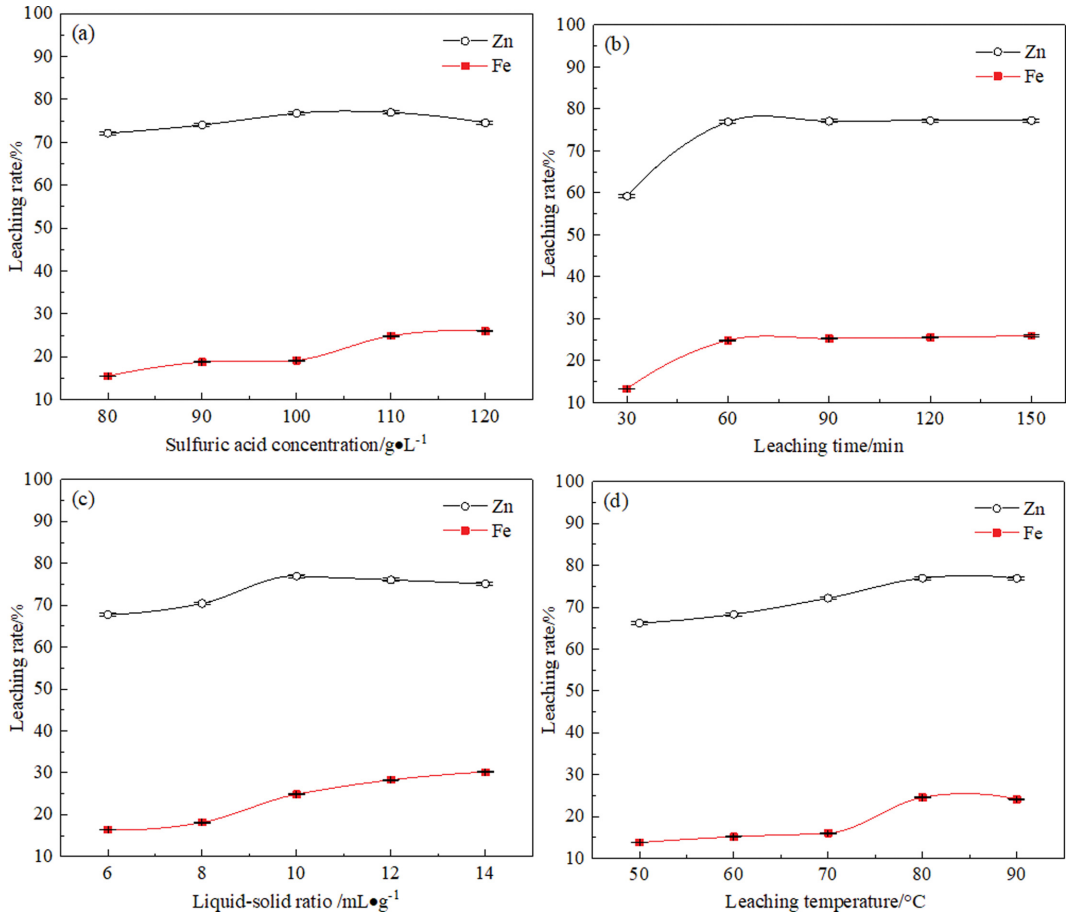

Fig. 8. Leaching regularities of roasting products under different leaching conditions: (a) leaching temperature is 80 °C, leaching time is 60 min, liquid-solid ratio is 10 : 1 mL g^{-1}, and stirring speed is 400 rpm; (b) leaching temperature is 80 °C, sulfuric acid concentration is 110 g L^{-1}, liquid-solid ratio is 10 : 1 mLg^{-1}, and stirring speed is 400 rpm; (c) leaching temperature is 80 °C, leaching time is 60 min, acid concentration is 110 g L^{-1}, and stirring speed is 400 rpm; (d) leaching time is 60 min, acid concentration is 110 g L^{-1}, liquid-solid ratio is 10 : 1 mLg^{-1}, and stirring speed is 400 rpm.

However, with the continuous prolongation of leaching time, hydrogen ions in the leaching solution were gradually consumed, which reduced the leaching rate, and the zinc and iron leaching rates did not increase significantly. The extension of leaching time did not significantly improve the zinc leaching rate, and the optimal zinc leaching time was 60 min.

Fig. 8(c) shows the influence of liquid-solid ratio on the leaching rates of zinc and iron from BFD sulfate roasting products. From Fig. 8(c), with an increase in the liquid-solid ratio, the overall zinc leaching rate showed a trend of first increasing and then decreasing, but the change range was small, whereas the leaching rate of iron showed a continuous increase trend. When the liquid-solid ratio was 10 : 1 mLg^{-1}, the maximum zinc leaching rate reached 76.94%. If the liquid-solid ratio was too small, the reaction between zinc and acid in the calcined product was incomplete, so that the zinc leaching rate was low. The zinc leaching rate increased gradually with an increase in the liquid-solid ratio, then the trend of gradually increased slowly, mainly is the increase in liquid-solid ratio contact surface of the solid particles and solution, to improve the liquidity of the leaching system, intensifying the tiny particles in the process of leaching movement and collision, so as to promote the reaction, but the liquid-solid ratio was too large and made the follow-up of leachate recycling process difficult. Based on a comprehensive analysis, 10 : 1 mLg^{-1} was selected as the optimal liquid-solid ratio.

Fig. 8(d) shows the influence of leaching temperature on the leaching rates of zinc and iron in the products of BFD sulfate roasting. From Fig. 8(d), the leaching temperature significantly influenced the zinc leaching rate, and when the leaching temperature increased to 80 °C, the zinc leaching rate was the highest; then with an increase in temperature, the zinc leaching rate did not increase significantly, because with an increase in leaching temperature the leaching reaction speed would increase correspondingly, and the increase in temperature decreased the solution viscosity, which is conducive to the diffusion of reactants and products in the reaction process. The higher the reaction temperature, the more volatile the acid solution; in addition, the consumption of hydrogen ions would reduce the acidity of the leaching solution, resulting in a decrease in zinc leaching rate. Therefore, to increase the zinc content in the leaching solution, the leaching temperature should be controlled as much as possible. In summary, 80 °C could be selected as the optimal leaching temperature.

Table 2. Comprehensive test results under optimized conditions (leaching rate %)

Number	Zinc leaching rate	Iron leaching rate
1	84.37	24.59
2	85.02	24.36
3	84.62	24.82
4	84.28	24.26
Average	84.57	24.51
Standard deviation	0.2868	0.2165

Through the single-factor experiments, a better process for separating zinc and iron by BFD roasting-leaching was obtained. Under the conditions of a roasting temperature of 600 °C, molar ratio of ferric sulfate to zinc ferrite of 1.2 : 1, roasting time of 60 min, sulfuric acid concentration of 110 g L^{-1}, leaching temperature of 80 °C, leaching time of 60 min, liquid-solid ratio of 10 : 1 mLg^{-1}, and stirring speed of 400 rpm, the separation effect of zinc and iron in BFD is better. To verify the stability of element leaching under these roasting-leaching conditions and the accuracy of optimized conditions, four groups of comprehensive tests were conducted; the results are summarized in Table 2. From the table, under the optimized conditions, the zinc and iron leaching rates were relatively stable, and the leaching rate fluctuated slightly. Our technique is an effective method for separating BFD and realizing the recycling of valuable metals.

5. Kinetics Analysis of Zinc Leaching Process

In the process of leaching zinc and iron by adding sulfuric acid to the products from the roasting of BFD ferric sulfate, the following reactions occurred:

$$ZnSO_4+2H^+\rightarrow Zn^{2+}+SO_4^{2-}+H_2O \quad (6)$$

$$Fe_2O_3+6H^+\rightarrow 2Fe^{3+}+3H_2O \quad (7)$$

The leaching process can be described as follows. Sulfuric acid diffuses to the surface of the roasted product particles through the diffusion layer and then further diffuses to the interior. Then, sulfuric acid reacts with the roasted product, which further diffuses from the product layer to the solution. As the reaction proceeds, the particle size of the reactants gradually decreases, which is a typical solid-liquid reaction; the reaction can be described by the shrinking nucleus model [34]. Shrink nucleus theory suggests that the reaction process comprises reactants and products in the reaction system, including liquid phase mass transfer, solid film diffusion, and interfacial chemical reaction. Under the condition of high-speed agitation, the influence of liquid mass transfer on the leaching rate is negligible, so the leaching rate is mainly determined by two steps: solid film diffusion and interface chemical reaction [35].

If the reaction is mainly controlled by chemical reaction, the reaction rate follows the following equation:

$$1-(1-R)^{1/3}=k_1t \quad (8)$$

If the reaction rate is controlled by solid film diffusion, the reaction rate follows the following equation:

$$1-2R/3-(1-R)^{2/3}=k_2t, \quad (9)$$

where R is the zinc leaching rate; k_1 is the rate constant of chemical reaction; k_2 is the diffusion velocity constant; T is the reaction time.

5-1. Influence of Leaching Temperature on Reaction Rate

When the sulfuric acid concentration was 110 gL^{-1}, leaching time was 1 h, liquid-solid ratio was 10 : 1 mLg^{-1}, stirring speed was 400 rpm, the leaching process of zinc at 50 °C, 60 °C, 70 °C, and 80 °C was studied, and the zinc leaching rate R corresponding to the leaching time t at different temperatures was recorded and calculated. The values of $1-(1-R)^{1/3}$ and $1-2R/3-(1-R)^{2/3}$ were calculated, and their relationships were plotted (Fig. 9).

Fig. 9 shows the leaching temperature diffusion model, indicating a good linear relationship with leaching time. The results show that solid membrane diffusion was more suitable for describing the leaching process of zinc in the BFD roasting product to describe the reaction speed, through dynamic curve calculated under different reaction temperatures zinc leaching reaction rate constant

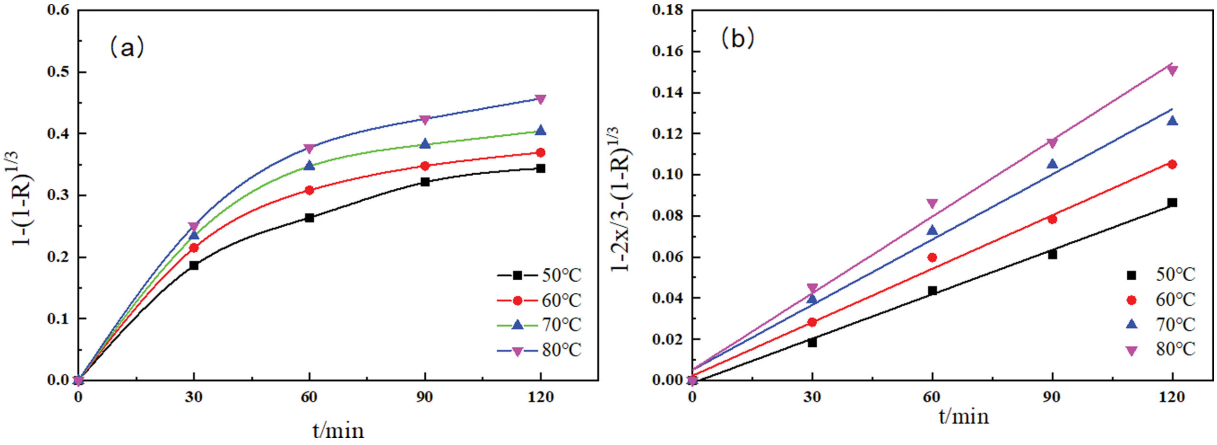

Fig. 9. Leaching kinetics curves of zinc from roasting products of BFD at different temperatures, sulfuric acid concentration is 110 gL^{-1}, leaching time is 1 h, liquid-solid ratio is 10 : 1 mLg^{-1}, stirring speed is 400 rpm, the leaching process of zinc at 50 °C, 60 °C, 70 °C, and 80 °C.

Table 3. Rate constants of zinc leaching at different temperatures

T/°C	50	60	70	80
Rate constants/min^{-1}	0.000719	0.000867	0.00106	0.00124
R^2	0.995	0.992	0.986	0.991

(Table 3).

From Table 3, the value of chemical reaction rate constant k gradually increased with the increase in reaction temperature, because the reaction was endothermic, and the increase in temperature was conducive to the reaction as well as accelerated the reaction.

In general, when the apparent activation energy was between 8 and 20 kJ/mol, the reaction was in the controlled region of solid film diffusion, i.e., the leaching rate was determined by the slowest diffusion rate [36]. The apparent activation energy of the leaching reaction can be calculated according to the Arrhenius equation, and the integral expression of the reaction rate can be expressed as follows:

$$\ln k = -\frac{E}{RT} + \ln A, \quad (10)$$

where k represents the reaction rate constant; E is the apparent activation energy, $kJmol^{-1}$; T is the thermodynamic temperature, K; R represents the ideal gas constant with a value of 8.314 J $mol^{-1}K^{-1}$; A represents the pre-exponential factor, and lnA is the integral constant.

The internal diffusion control model was used to plot the lnk versus 1/T of the zinc leaching process in the BFD roasting products at different temperatures; the fitting results are shown in Fig. 10.

According to Figs. 9 and 10, the leaching process of zinc from the roasted products of BFD ferric sulfate has a good fitting effect with the internal diffusion model at different thermodynamic temperatures. The apparent activation energy E of the leaching process was 17.4 $kJmol^{-1}$, and the reaction rate constant was 0.47. Results indicate the reaction activation energy surface leaching process is controlled by internal diffusion and affects the leaching rate of mainly for the sample size and leaching liquid concentration. Reducing the sample size can increase the specific surface area, reduce fixed film thickness, shorten leaching time, so as to speed up the rate of leaching process which can improve the crushing process, reduce the calcined product granularity. Maintaining a certain acid concentration would increase the concentration difference as well as promote early diffusion, and the decrease in solid-liquid ratio would increase the contact area as well as promote diffusion.

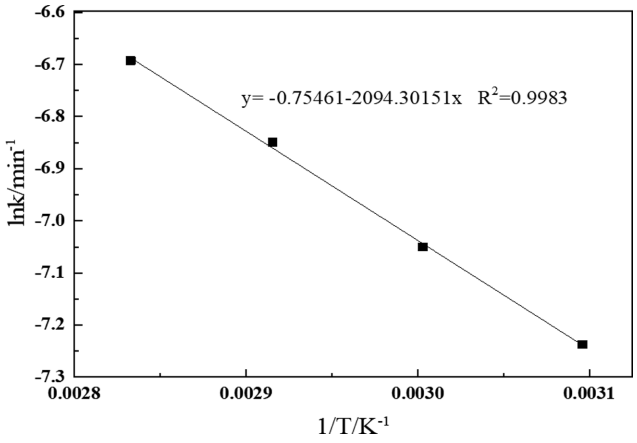

Fig. 10. Fitting curve of lnk and 1/T in zinc leaching process.

5-2. Influence of Leaching Acidity on Reaction Rate

To verify that the limiting process of zinc leaching from BFD roasting products was leaching at 80 °C, liquid-solid ratio of 10 : 1 mLg^{-1}, and sulfuric acid concentration of 80, 90, 100, and 110 gL^{-1}, the leaching rate R corresponding to leaching time t at different temperatures was analyzed. The leaching time of $1-2R/3-(1-R)^{2/3}$ was fitted; the results are shown in Fig. 11. The leaching rate constants of zinc in the roasting products of BFD sulfuric acid with different acidities are listed in Table 4.

From Fig. 11 and Table 4, leaching of zinc from BFD roasting products at different sulfuric acid concentrations conformed to the unreacted core model, with good linear correlation coefficients around 0.99, and diffusion was the restrictive step. With the increase

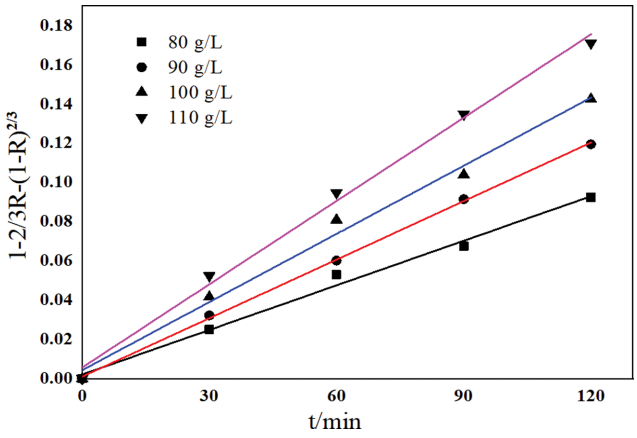

Fig. 11. Leaching kinetics curve of zinc from roasting products of BFD at different sulfuric acid concentrations. Leaching temperature is 80 °C, liquid-solid ratio is 10 : 1 mLg^{-1}, and sulfuric acid concentration is 80, 90, 100, and 110 gL^{-1}.

Table 4. Rate constants of zinc leaching at different sulfuric acid concentrations

Sulfuric acid concentrations/($g \cdot L^{-1}$)	80	90	100	110
Rate constants/min^{-1}	0.000757	0.000994	0.00116	0.00141
R^2	0.989	0.999	0.989	0.992

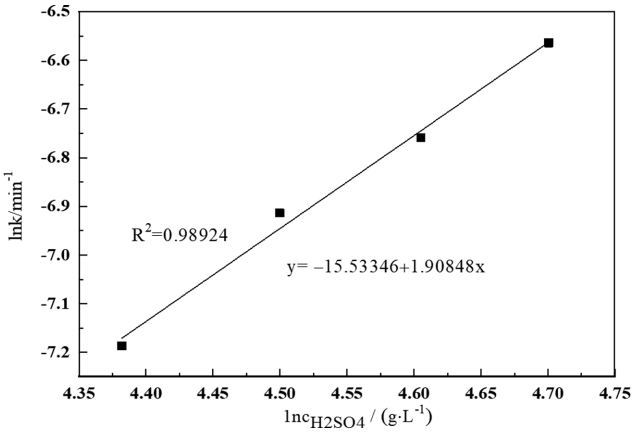

Fig. 12. Apparent reaction order of zinc leaching from BFD roasting products at different acidity levels.

in the concentration of sulfuric acid, zinc leaching rate constant increased in the process, showing that the current increase in the concentration of sulfuric acid can accelerate the leaching reaction, which is beneficial to the improvement of the zinc leaching rate, but diffusion will no longer be a restricted link, which indicates the leaching rate of acid concentration of elements increase is less. The liquid-solid ratio was 110 gL^{-1} in the combined leaching process. The leaching process mechanism at different acidities agreed with the leaching process at different temperatures. To further obtain the apparent reaction order of the leaching process, lnk was used to plot $\ln C_{H2SO4}$ (Fig. 12), which shows a good linear correlation; the correlation coefficient was 0.989, and the slope of the fitting line was 1.908, which was the apparent reaction order of the leaching reaction.

CONCLUSIONS

Sulfate roasting-acid leaching method can separate zinc and iron from BFD, which is an effective strategy for comprehensively using BFD. Through the study of the material transformation, surface morphology, leaching process, and leaching kinetics in the reaction process, the following conclusions are drawn.

1) The BFD mainly contains ferric oxide, carbon, and zinc ferrite. The thermodynamics analysis of the BFD sulfate roasting process showed that the conversion of zinc ferrite to zinc sulfate could be realized when the roasting temperature range was 500-730 °C, which was convenient for zinc leaching.

2) A better roasting condition could be obtained when the roasting temperature was 600 °C, roasting time was 60 min, and ratio of ferric sulfate was 1.2 : 1. Under the conditions of sulfuric acid concentration of 110 gL^{-1}, liquid-solid ratio of 10 : 1 mL g^{-1}, leaching time of 1 h, stirring speed of 400 rpm, and leaching temperature of 80 °C, the zinc and iron leaching rates were 84.57% and 24.51%, respectively.

The leaching process of zinc from BFD sulfate roasting products agreed with the unreacted core model, with the internal diffusion as the restrictive step.

The separation of zinc and iron by roasting BFD with ferric sulfate was efficient and reasonable for resource usage without introducing other impurities in the leaching reaction and product generation.

ACKNOWLEDGEMENTS

The authors gratefully acknowledged the National Natural Science Foundation of China (No. 51904223); Young Talents Support Program of the Science and Technology Association of Shaanxi, China (No. 20190603); Shaanxi Province Key R&D General Project-Industrial Field, China (No. 2021GY-128); Innovative Research and Development Institute of Guangdong (No. 2018B090902009).

REFERENCES

1. F. Zhang, S. Z. Zhang, G. P. Luo, Z. P. Hao and J. Q. Wang, *Iron and Steel*, **46**, 7 (2011).
2. G. L. Jia and B. H. Zhang, *China Metall.*, **17**, 18 (2007).
3. D. L. Zheng, S. L. Liu, Q. Zhang, S. H. Luo, G. H. Wang and M. Su, *Chin. J. Nonferrous Met.*, **43**, 57 (2014).
4. L. Shi, R. H. Chen and R. Y. Wang, *China Resources Comprehensive Utilization*, **27**, 19 (2009).
5. Z. L. Cheng, Z. T. Tan, Z. G. Guo, J. Yang and Q. W. Wang, *Renew. Sust. Energ. Rev.*, **131**, 110034 (2020).
6. Y. J. Tan, Y. F. Guo, T. Jiang, Z. Q. Xie, W. Chen and X. D. Liu, *Multipurpose Utilization of Mineral Resources*, **7**, 44 (2017).
7. W. G. Fu, *Iron and Steel*, **45**, 10 (2010).
8. J. Heubes, *Chin. J. Nonferrous Met.*, **24**, 511 (2014).
9. G. M. Jiang, B. Peng, Y. J. Liang, L. Y. Chai, Q. W. Wang, Q. Z. Li and M. Hu, *Trans. Nonferrous Met. Soc. China*, **27**, 1180 (2017).
10. S. Kelebek, S. Yörük and B. Davis, *Miner. Eng.*, **17**, 285 (2004).
11. K. Cao, L. G. Hu and Y. M. Jia, *Metallurgical Power*, **5**, 16 (2006).
12. C. J. Liu and E. Z. Hu, *Chin. Metall.*, **9**, 40 (2004).
13. S. Gerolf and J. E. Bonestell, *Iron and Steel Engineer*, **73**, 87 (1996).
14. W. Puta, *Steel Times*, **217**, 194 (1989).
15. X. J. Hu, T. Guo and G. Z. Zhou, *J. Iron Steel Res. Int.*, **23**, 1 (2011).
16. H. C. Xu, H. M. Zhou, Y. H. Qi and G. H. Xie, *Iron and Steel*, **47**, 89 (2012).
17. K. Y. Peng, Y. Zhou, L. S. Li, S. J. Wang, H. C. Wang and Y. C. Dong, *China Resources Comprehensive Utilization*, **6**, 8 (2005).
18. Y. Hara, N. Ishiwata and H. Itaya, *ISIJ Int.*, **40**, 231 (2000).
19. N. Standish and H. Labee, *Ironmaking and Steelmaking*, **69**, 486 (1992).
20. M. Crruells, A. Roca and C. A. Nunez, *Hydrometallurgy*, **31**, 213 (1992).
21. R. S. Zhu, Z. Wu, T. F. Yi and Z. Y. Xia, *Mining and Metallurgical Engineering*, **32**, 103 (2012).
22. W. J. Bruckard, K. J. Davey, T. Rodopoulos, J. T. Woodcock and J. Italiano, *Int. J. Miner. Process.*, **75**, 1 (2005).
23. X. Luo, C. Wei, X. Li, Z. Deng and G. Fan, *Hydrometallurgy*, **197**, 105458 (2020).
24. Y. C. Li, S. N. Zhuo, B. Peng, X. B. Min, H. Liu and Y. Ke, *J. Clean. Prod.*, **263**, 121468 (2020).
25. X. B. Min, G. H. Jiang, Y. Y. Wang, B. S. Zhou, K. Xue, Y. Ke, Q. J. Xu, J. W. Wang and H. C. Ren, *J. Cent. South Univ.*, **27**, 1186 (2020).
26. X. B. Min, B. S. Zhou, Y. Ke, L. Y. Chai, K. Xue, C. Zhang, Z. W.

Zhao and C. Shen, *Appl. Surf. Sci.*, **371**, 67 (2016).
27. B. Xu, L. Yu, X. Zhao, H. Wang, C. Wang, L. Y. Zhang and G. L. Wu, *J. Colloid Interface Sci.*, **584**, 827 (2021).
28. W. Q. Luo, X. Liu, Y. Q. Yang, H. He and B. Gao, *Chin. J. Environ. Eng.*, **6**, 317 (2012).
29. Z. Youcai and R. Stanforth, *J. Hazard. Mater.*, **80**, 223 (2000).
30. Y. Zhao and R. Stanforth, *Chin. J. Nonferrous Met.*, **12**, 174 (2004).
31. J. Heubes, *Chin. J. Nonferrous Met.*, **24**, 511 (2014).
32. M. Li, B. Peng, L. Y. Chai, N. Peng, H. Yan and D. K. Hou, *J. Hazard. Mater.*, **238**, 323 (2012).
33. D. Q. Zhu, D. Wang, J. Pan, H. Y. Tian and Y. Xue, *Powder Technol.*, **380**, 273 (2020).
34. Z. X. Liu, Z. L. Yin, H. P. Hu and Q. Y. Chen, *Trans. Nonferrous Met. Soc. China*, **22**, 2822 (2012).
35. L. Tao, L. Wang, K. Yang, X. Wang, L. Chen and P. Ning, *RSC Adv.*, **11**, 5741 (2021).
36. Q. H. Gui, M. L. Khan, S. X. Wang and L. B. Zhang, *Hydrometallurgy*, **196**, 105426 (2020).